SOME COMPUTATIONAL PROBLEMS IN MICROFLUIDICS.

S. Tancogne, Ch.-H. Bruneau, Th. Colin

Institut de Mathématiques de Bordeaux, University of Bordeaux and INRIA, project MC2, 351 cours de la Libération, 33405 Talence cedex.

and

A. Colin, P. Guillot, M. Joanicot,

Rhodia Laboratoire du Futur, Unité Mixte Rhodia-CNRS, Université Bordeaux I, 178 Avenue du Docteur Schweitzer, 33608 Pessac, France

Corresponding author: Thierry Colin, colin@math.u-bordeaux1.fr

1 Introduction

The aim of this paper is to present some results of flow simulations in microfluidics. Microfluidics is characterized by the manipulation of very small volumes of fluids of the order of the nanoliter. The spacial scales are below the millimeter and typically the sections of the microchannels are $100\mu m \times 100\mu m$ and are $5cm$ long. It is possible to handle very stable flows (co-flows, droplets...). From the modeling point of view, the velocity are around 1 cm per second and the Reynolds number is quite small (smaller than 1) in general. Inertial effects can usually be neglected. However, surface tension phenomena are predominant and from the numerical point of view, it is required to have very precise computations in the case of multifluid flows in order to have predictive results.

In this context, numerical simulations are used in order to understand the structure of the flows but also to get quantitative informations starting from experiments. An example is given in the next section, concerning a viscosimeter.

The models used in this paper are the following.

Navier-Stokes equations are used for the hydrodynamic. The interface is transported by the velocity field and the surface tension effects are added. The no-slip boundary conditions are set on the rigid walls. This condition is obviously not valid and one has to use more subtle conditions in order to take into account the movement of the contact line (see [2]) for example. However in

this work, the investigations are restricted to homogeneous Dirichlet boundary conditions or to Fourier-type boundary conditions. Fluid i (for i=1or 2) has viscosity η_i, density ρ_i, pressure p_i and velocity U_i in $\Omega_i(t)$. The steady Navier-Stokes equations read

$$\rho_1 U_1 \cdot \nabla U_1 - \eta_1 \Delta U_1 + \nabla p_1 = 0 \text{ and } \nabla \cdot U_1 = 0 \tag{1.1}$$

$$\rho_2 U_2 \cdot \nabla U_2 - \eta_2 \Delta U_2 + \nabla p_2 = 0 \text{ and } \nabla \cdot U_2 = 0 \tag{1.2}$$

The equation for U_i is valid in the spacial domain $\Omega_i(t)$ that depends on time t. Let us denote by $I(t)$ the interface at time t. We have to add transmission conditions at the interface. These conditions are:
i) Continuity of the velocity field on $I(t)$: $U_1 = U_2$.
ii) Jump of the normal part of the stress tensor:

$$\sigma_1 \cdot \vec{n} = \sigma_2 \cdot \vec{n} + \frac{T}{R}\vec{n} \tag{1.3}$$

where σ_i is the stress tensor of the fluid i given by

$$\sigma_i = -p_i \mathbf{I} + 2\eta_i D(U_i),$$

with $\mathbf{I}$ is the identity matrix, $D(U_i)$ the deformation rates tensor $D(U_i) = \frac{\nabla U_i + \nabla U_i^t}{2}$. and $\vec{n}$ the normal vector to the interface, R is the mean curvature and T is the surface tension coefficient.
We describe the displacement of the interface by imposing that the velocity of the interface is equal to that of the fluid.
With a level-set description, we consider the function $\varphi(t, x, y, z)$ such that at $t = 0$

$$\varphi(0, x, y, z) < 0 \text{ in fluid 1}$$

$$\varphi(0, x, y, z) > 0 \text{ in fluid 2}$$

The velocity field U is defined by $U = U_1$ in fluid 1 and $U = U_2$ in fluid 2 and the motion of the level-set function is given by

$$\partial_t \varphi + U \cdot \nabla \varphi = 0,$$

and therefore

$$\varphi(t, x, y, z) < 0 \text{ in fluid 1}$$

$$\text{and } \varphi(t, x, y, z) > 0 \text{ fin luid 2}$$

and the interface is the level set $\varphi = 0$.

The Navier-Stokes equations can be rewritten

$$\rho U \cdot \nabla U = 2\nabla \cdot (\eta D(U)) + \nabla p - \frac{T}{R}\delta_I \vec{n},$$

$$\nabla \cdot U = 0,$$

where δ_I is the Dirac mass on the interface $I(t)$.

We consider typically two kinds of geometries. The first one is a "T"-junction as show in fig. 1 for which the fluids are injected in the small branches of the "T".

The second configuration is the flow of a jet in a cylindrical channel as in fig. 2 for which there is a internal fluid and an external one.

The content of this paper is the following : in the next section we present the principle of the viscosimeter. In section 3, we present the analysis of the stability of a jet in a microchannel. And in section 4, we present 3D numerical simulations for the formation of droplets.

2 Viscosimeter

As recalled in the introduction, the order of magnitude of the velocities is the cm/s, while the characteristic length are around $100\mu m$. The Reynolds numbers are therefore of the order of unity and one can have very stable flows. An example of such flows is given in the photo of fig. 3. Two non-miscible fluids are injected in the channel via the "T"-junction. We use the geometry indicated in fig. 1 and the idea is to use this geometry to obtain some informations concerning the fluids. The fluids are injected by the small branches of the "T" and the coflow becomes steady in the long branch of the "T". So, knowing the position of the interface, the flow rates of each fluids and the viscosity of one fluid, is it possible to compute the viscosity of the other fluid? Assuming that both fluids are Newtonian, we give two viscosities, compute the velocity fields, then the flow rates. One then iterates the procedure with different sets of viscosity in order to obtain the right value of the flow rates.

On a cartesian mesh, we consider the flow in an infinite channel where z denotes the coordinate along the channel while $X = (x, y)$ denotes the transverse coordinates. We assume that we have a steady-state flow that is invariant under the action of translations parallel to the direction of the channel. It implies that the following properties are satisfied:
•The pressure is constant in the transverse plane, the gradient of pressure is in the direction of the channel and is constant,
•The velocity field is longitudinal and depends only on the transverse variable,
•The interface is an arc of a circle,

The fluid 1 has viscosity η_1, velocity $(0, 0, u_1)$ and occupies the spacial domain $\mathbb{R} \times \Omega_1$ while the fluid 2 has viscosity η_2, velocity $(0, 0, u_2)$ in domain $\mathbb{R} \times \Omega_2$.
In this case, the Navier-Stokes equations (1.1)-(1.2) reduce to the following set of elliptic equations:

$$-\eta_1 \Delta u_1 = \delta p \text{ in } \Omega_1,$$

$$-\eta_2 \Delta u_2 = \delta p \text{ in } \Omega_2,$$

where δp denotes the gradient of the pressure in the longitudinal direction.

We need to write the interface conditions in order to get some transmission conditions. The jump conditions on the normal part of the stress tensor leads in this context to:

$$u_1 = u_2 \text{ and } \eta_1 \partial_n u_1 = \eta_2 \partial_n u_2 \text{ on the interface.}$$

One can therefore obtain a global formulation for this set of equations. Let $u = u_i$ and $\eta = \eta_i$ in fluid i. The system reads

$$-div(\eta D(U)) = \delta p$$

in the domain and we impose the non-slip boundary condition $u = 0$.
Exemple of profile for a jet and a coflow are given in fig. 4 and 5. The results are compared to experiments and show a good agreement in [1].

One of the key issue from the practical point of view is to understand the formation of the jet and/or the co-flow, that means to be concerned with stability issues. From the numerical point of view, two approaches are possible. The first one is to perform a linear stability analysis (using the numerics at the end of the procedure in order to compute eigenvalues) or direct numerical simulations. The first approach as the advantage to be rapid but the main drawback is that nonlinear phenomena are not taken into account. The direct simulation is of course more precise but it is expensive in terms of computational times, specially for 3D cases. In the next section we present two examples of these approaches.

3 Stability of a jet.

The aim of this section is to present a linear analysis of the stability of a jet in the cylindrical geometry of fig. 2 and to recover phase diagrams of the kind of fig. 6 where the shape of the flow is indicated in terms of the internal (Q_i) and external (Q_e) flow rates. The breaking of a jet is known as the Rayleigh-Plateau instability.

The configuration is that of fig. 7. The radius of the cylinder is Re while that of the jet is Ri and the flow rate of the internal (resp. external) fluid is denoted by Q_i (resp. Q_e). We assume that the flow is axi-symmetrical. The velocity profile of the steady-state flow is indicated on fig. 7 and is of the form $(0, v(r))$ in cylindrical coordinates. We want to determine the stability of this flow and therefore we consider a perturbation ξ of the interface as indicated on fig.7.

We perform the linearization of the system (1.1)-(1.2) around the stationary solution $(0, v(r))$ and take the perturbation under the form $e^{-ikz}(u_r(t,r), u_z(t,r))$.

One gets the following equation on the auxilliary variable $Z_j(t,r) = u_r + \frac{1}{ik}\partial_r u_z$ ($j = 1$ for $0 \leq r \leq R_i$ and $j = 2$ for $R_i \leq r \leq R_e$):

$$\partial_r^2 Z_j(t,r) + \frac{1}{r}\partial_r Z_j(t,r) - \left(-ik\frac{\rho_j}{\eta_j}v(r) + \frac{1}{r^2} + k^2\right) Z_j(t,r) = 0. \qquad (3.4)$$

The incompressibility gives:

$$\partial_r u_r - iku_z = 0.$$

And therefore (3.4) leads to a fourth order equation on the radial velocity u_r.

The linearized equation for the position of the interface is

$$\partial_t \xi - ikv(R_i)\xi = u_r(R_i). \tag{3.5}$$

The jump conditions (1.3) give four linear matching conditions on u_r, $\partial_r u_r$, $\partial_r^2 u_r$, $\partial_r^3 u_r$ at $r = R_i$ involving ξ and the following straightforward result follows:

Proposition 3.1 *There exists $\alpha(k) \in \mathbb{C}$ such that $u_r(R_i) = \alpha(k)\xi$.*

Therefore, equation (3.5) reads

$$\partial_t \xi - ikv(R_i)\xi = \alpha(k)\xi,$$

and the sign of $Re(\alpha)$ gives the stability.
But the situation is a little more subtile. We first define some critical length:

$$\alpha_0 = \max_{\alpha(k)>0} \alpha(k) \text{ and } L_c = \frac{V_{fluid}}{\alpha_0}$$

where V_{fluid} is the maximum velocity of the fluid for the stationary flow. L_c is the length that is needed by the instability to grow. Therefore if the length L of the channel is larger that L_c the jet will be unstable; but if $L < L_c$ the jet will be stable even if the real part of α_0 is positive. The results are plotted in fig. 8. We have recalled the phase diagram obtained by P. Guillot et al. [4] and we have performed 3 simulations corresponding to 3 different surface tension coefficients. The physical one is represented by the +, the smallest one with triangle and the medium with the square. We have drawn the critical length, the frequency (that it the value $real(\alpha_0)$) and the more unstable wave-length (that is $1/k_0$ where $\alpha(k_0) = \alpha_0$). The external flow rate is fixed and we let vary the internal one. We see that the numerical results are coherent with the experiments, that when surface tension decreases, stability increases. One also remarks that the most unstable wave-length does not depend on surface tension.

On fig. 9, we fix the internal flow-rate and let vary the external one. Again, the physical case is drawn with + and the circle represent a smaller surface tension. We see that the curve of the critical length is not monotone. This is coherent with the phase diagram.

4 Droplets formation.

When the jet is not stable, one can observe the formation of droplets. This is an highly nonlinear phenomena that can not be described by the approach of the previous section. The only solution is to perform direct numerical simulations.

We implement numerically the level-set method. Let φ be the function defining the interface [5, 6, 7], the incompressible Stokes equations reads:

$$-div(2\eta D(U)) + \nabla P = \sigma\kappa\delta(\varphi)n,$$

$$\nabla \cdot U = 0,$$

where κ is the curvature given by $\kappa = \nabla \cdot n$ and $n = \frac{\nabla\varphi}{||\nabla\varphi||}$. The equations are discretized by a finite volume scheme using a staggered mesh as shown in fig. 10.

One still have to solve a transport equation for φ:

$$\partial_t\varphi + U \cdot \nabla\varphi = 0$$

and the weno 5 scheme [8] is used for the discretization.

In fig. 11 one can compare the experimental data with the numerical ones.

Depending on the flow rate, one can observe different shapes of droplets, for example plugs in fig.12.

The code is able to describe the formation of droplets, as shown in fig. 13.

5 Conclusion

We are able to predict numerically by a simple linear analysis the stability of a jet. The direct numerical simulations give us the main feature of the flows. We now have to make quantitative comparisons with experiments in a 3D geometry. For that purpose, we need to implement more reliable boundary conditions for the contact line problem.

References

[1] P. Guillot, P. Panizza, J.-B. Salmon, M. Joanicot, A. Colin, C.-H. Bruneau and T. Colin, *Viscosimeter on a Microfluidic Chip*, Langmuir 2006, 22, 6438-6445.

[2] W. Ren, W. E, *Bounday conditions for the moving contact line problem*, Physics of fluids 19, 022101 (2007).

[3] C. Galusinski and P. Vigneaux, *Level-Set method and stability condition for curvature-driven flows*, C. R. Acad. Sci. Paris, Ser. I 344 (2007) 703708.

[4] P. Guillot, Thesis, University Bordeaux 1, 2006.

[5] S. Osher, Stanley and J.A. Sethian, *Fronts propagating with curvature-dependent speed: algorithms based on Hamilton-Jacobi formulations*, J. Comput. Phys., 79, (1988), 12–49.

[6] S. Osher and R. Fedkiw, *Level Set Methods ans Dynamic Implicit Surface*, Applied Mathematical Sciences 153, Springer, 2003.

[7] M. Sussman, P. Smereka, S. Osher. *A level set approach for computing solutions to incompressible two-phase flow*, J. Comput. Phys. 114 (1994) 146–159.

[8] G.-S. Jiang and D. Peng, *Weighted ENO schemes for Hamilton-Jacobi equations*, SIAM J. Sci. Comput., 21, (2000), 2126–2143.

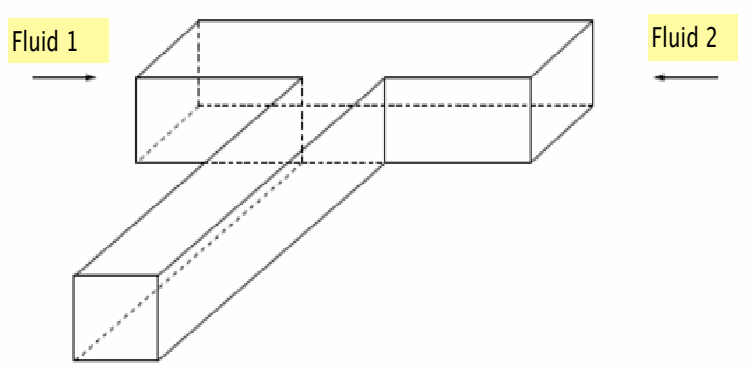

Figure 1: A "T" junction geometry

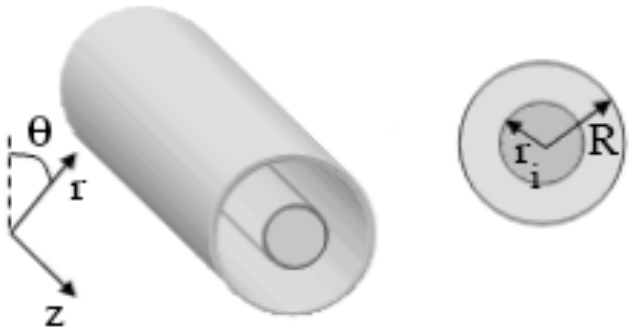

Figure 2: A cylindrical geometry

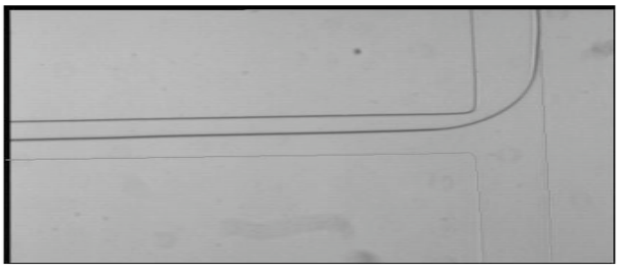

Figure 3: A coflow in a "T"-junction.

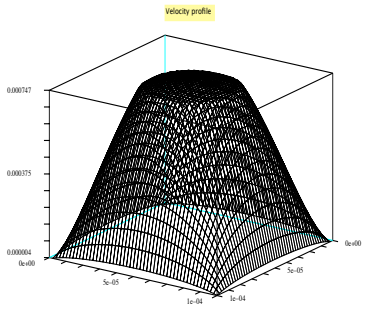

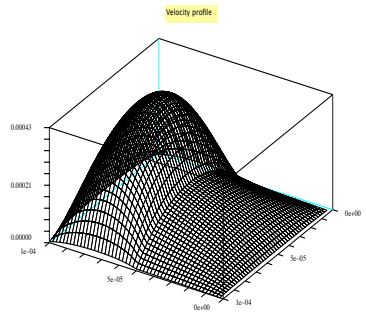

r profile for a jet.

Figure 5: Velocity profile for a co-flow.

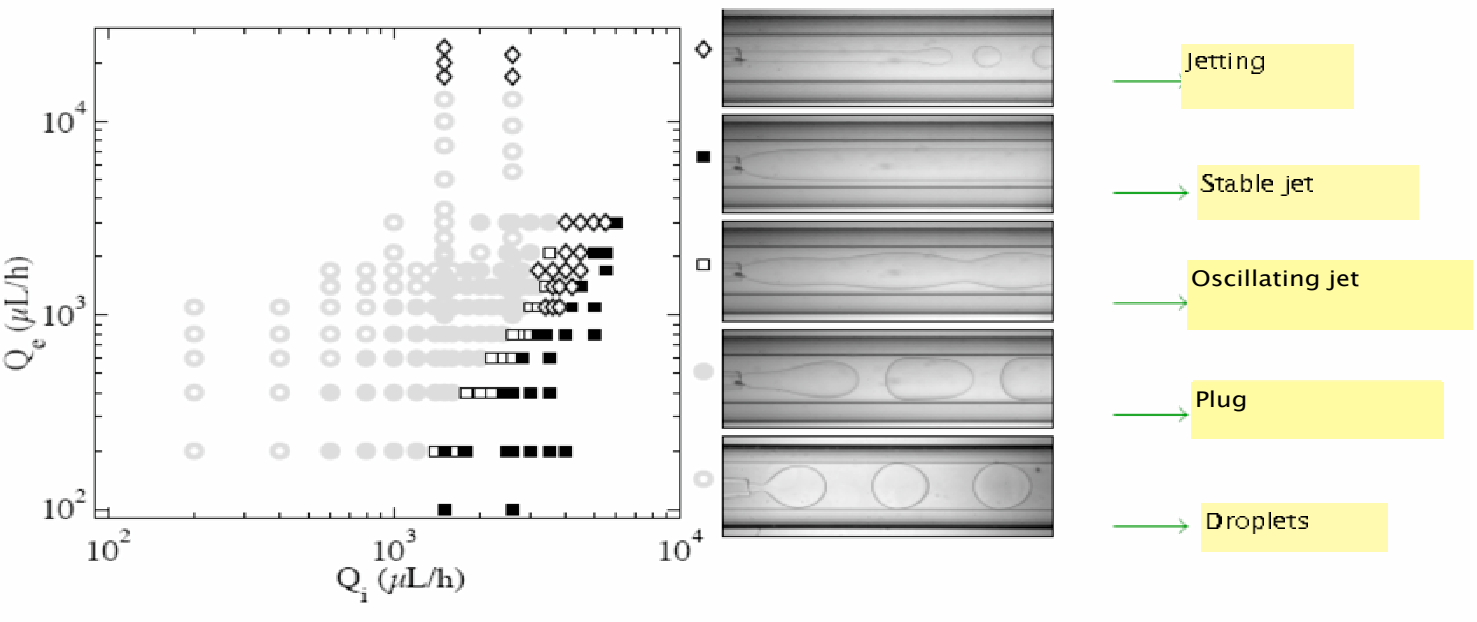

[4] P. Guillot, A. Colin A. Utada, A. Adjari, Stability of jet in confined pressure-driven biphasic flows at low reynolds number.

Figure 6: Phase diagram in the cylindrical geometry

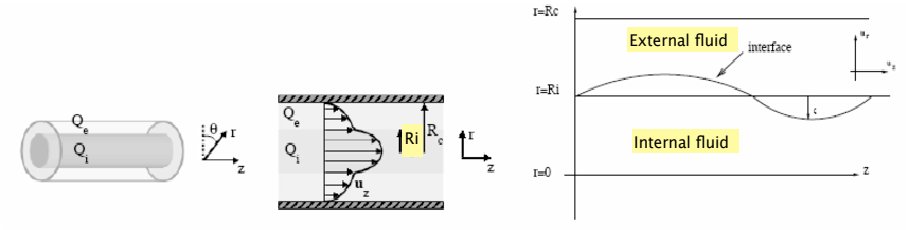

Figure 7: Configuration of the flow in the cylindrical geometry

- $Q_e = 1000 \mu L/h$ Critical length, frequency and most unstable wave-length with respect to Qi for different surface tensions

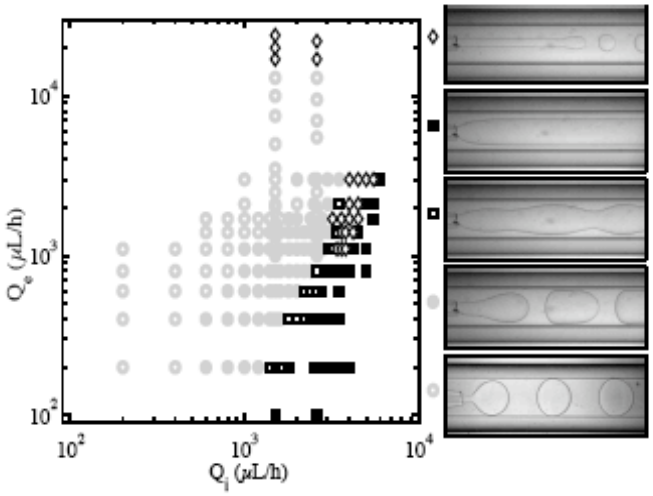

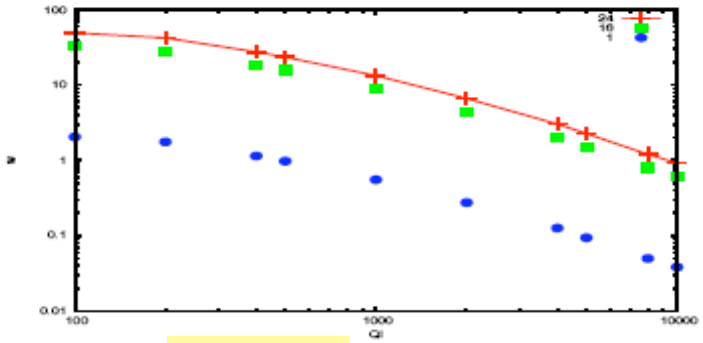

Frequency in s^{-1}.

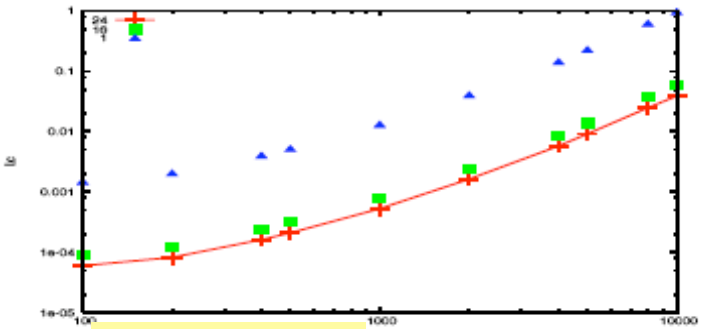

Critical length in m.

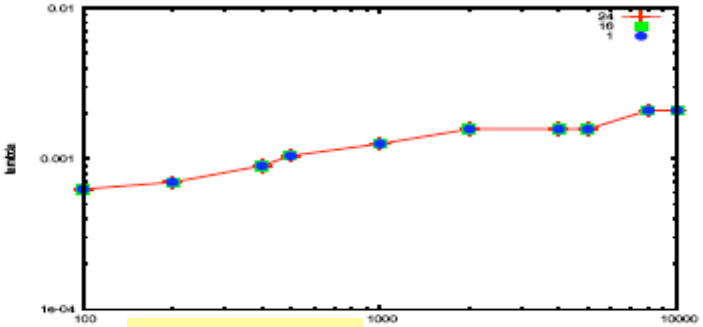

Wave-length in m.

Figure 8: Numerical results at fixed external flow rate.

- $Q_i = 1000 \mu L/h$ Critical length, frequency and most unstable wavelength with respect to Qe.

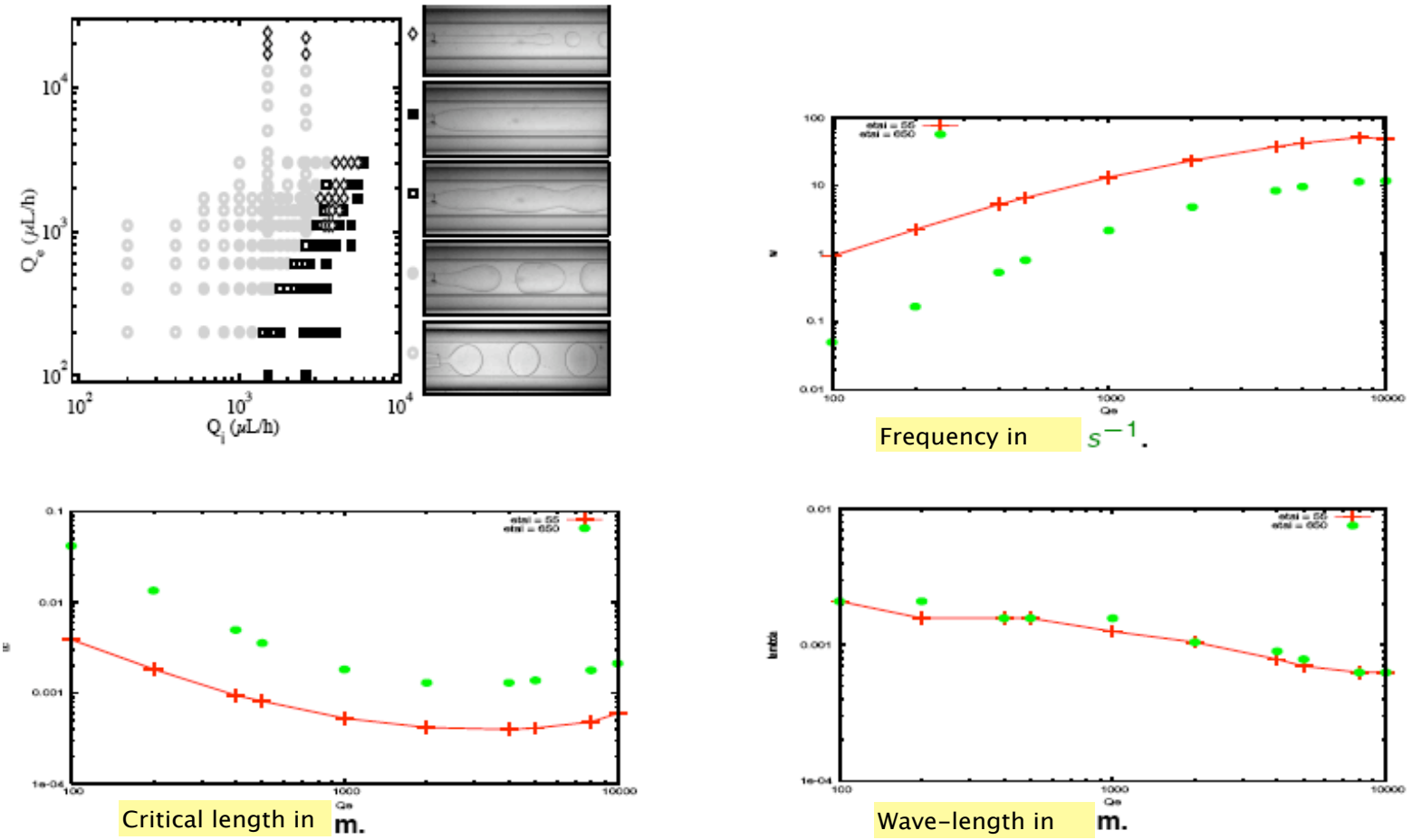

Figure 9: Numerical results at fixed internal flow rate.

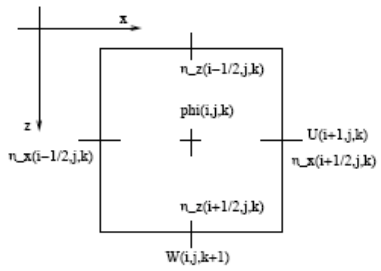

Figure 10: A staggered mesh. U and W denote respectively the first and third component of the velocity, η_x and η_z the values of the viscosity that are used in the finite volume scheme.

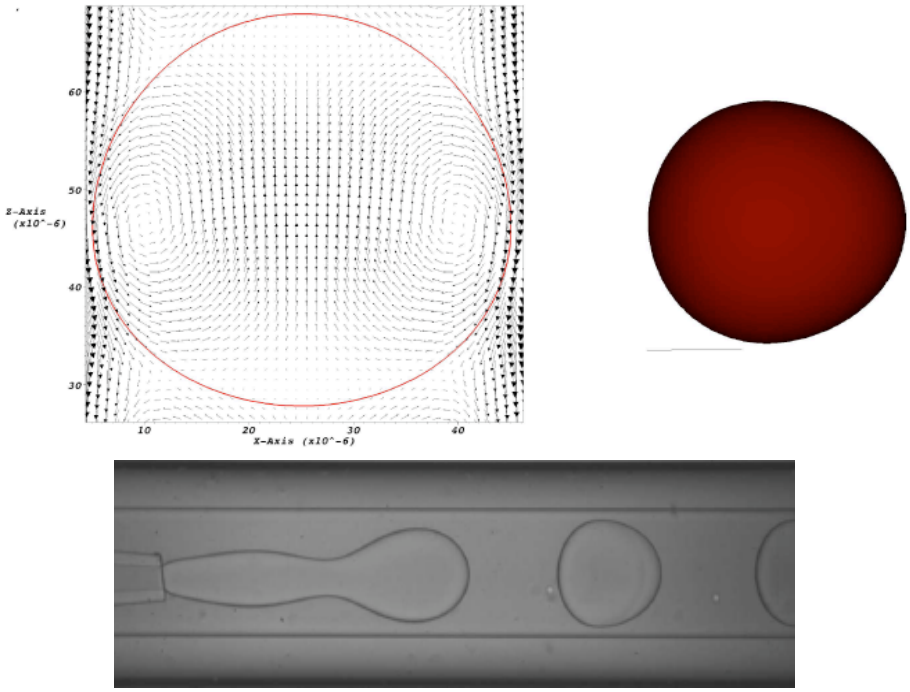

Figure 11: Numerical shape of a droplet and velocity field. An experimental picture with similar values.

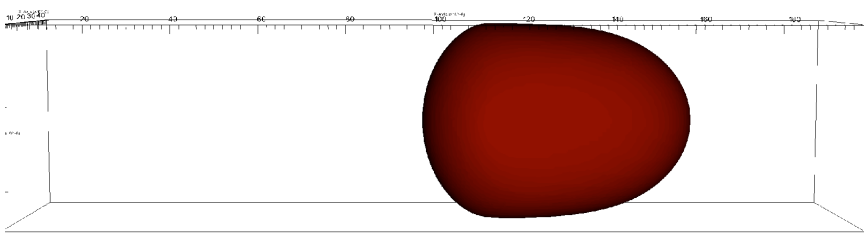

Figure 12: Numerical simulation of a plug.

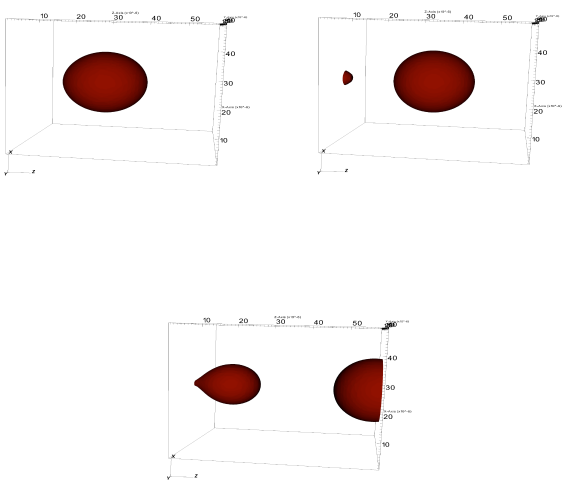

Figure 13: Numerical simulation of the formation of a droplet.